

# Application of an Innovative Precise Integration Method in Solving Equilibrium Equations of Motion for Structural Dynamic Problems

**Chiun-lin Wu**

*National Center for Research on Earthquake Engineering, Taipei City, Taiwan*

**Ching-Chiang Chuang**

*Department of Civil Engineering, Chung Yuan Christian University, Chungli City, Taiwan*



## SUMMARY:

A very popular approach to conduct structural dynamic response analysis is to first formulate its dynamic equilibrium equations of motion, and then employ a step-by-step time integration scheme to solve the equations such that dynamic equilibrium is satisfied at discretized time instants. The selection of time step size depends on the features of the time integration approach, and should consider its numerical stability, desired accuracy, predominant frequencies of the analyzed structure as well as the major characteristics of the external loadings. In case of high dominant structural frequencies or dramatic loading variations, a sufficiently small time step is usually required to achieve satisfactory numerical accuracy. The authors studied two major cases of employing both force and momentum equations of motion together with a so-called "Precise Integration Method" to solve for dynamic structural response. Compared with most of the conventional numerical integration methods in the literature, the proposed method is found less insensitive to the selection of time step size in case of impulsive loading and is able to provide superior numerical stability and accuracy. This study also investigates the advantage in the use of a nonlinear polynomial function in describing the variation of loading momentum within an integration time step, which further helps loosen the constraint of time step size required for better accuracy.

*Keywords: precise integration, numerical stability, accuracy, high-frequency dissipation, spurious resonance*

## 1. INTRODUCTION

It is well known that mechanical governing equations describing dynamic engineering problems basically take the form of partial differential equations. To solve the equations, most numerical solution methods (e.g., finite element method, finite difference method, etc.) start with a set of simultaneous ordinary differential equations (ODE) through discretized spatial coordinate, and employ a direct integration method to obtain the final solution. In the field of structural dynamics, for instance, the original Newmark's, Wilson- $\theta$ , and Houbolt methods are very popular methods that can be categorized as implicit methods; on the other hand, the modified Newmark's and central difference methods belongs to the group of explicit methods. In either way, the time step size should be carefully selected in integration to ensure numerical stability as well as accuracy. Taking explicit methods for example, the selection of the time step size is more rigorous and usually depends on the highest dominant frequency of the structural system being analyzed. Such a small time step is usually set to satisfy the requirement of numerical stability with a tradeoff of increasing computational efforts. In addition, the calculated fundamental periods and vibration modes highly depend on the selected structural model that is used to describe a real structural system. In some cases, the higher vibration modes may not represent the real response of the original structural system, and will reduce the computational accuracy, and inevitably affect the confidence in interpreting numerical results obtained. As such, it is a common concern of many researchers how to develop a reliable integration algorithm for solving simultaneous ODEs and having the capability of dissipating fictitious high frequency response at the same time.

Subbaraj and Dokainish (1989) presented a thorough review on direct time integration methods developed before 1989. One can also refer to Hughes (1987) for a number of popular integration

methods in the literature. In addition to finite difference methods, there are other schemes using finite element concept to solve time integration problems, e.g., time-discontinuous Galerkin method, which is capable of doing integration in one single time step with self-starting initial guess, and provides higher accuracy and better numerical stability through dissipative integration scheme eliminating high frequency noise (Chien et al., 2003). In order to solve simultaneous ODEs in a more efficient manner, Zhong and Williams (1994) proposed the High Precision Direct-L (HPD-L) method, which expressed the analytical homogeneous solution of the simultaneous ODEs in a fourth order Taylor series expansion to be integrated using the famous power-of-two algorithm, and in the meantime the external loading force was represented by a segmented piecewise-linear force history, in which the time step size was mainly determined by the degree of nonlinearity of the external force history, while the influence of the natural periods of the analyzed structure on solution accuracy was found insignificant. Lin et al. (1995) and Shen et al. (1995) adopted the same concept with the loading force history represented in the form of the famous Fourier series expansion and this approach was usually referred to as High Precision Direct-F (HPD-F) method in the literature, which oftentimes was implemented through parallel computing techniques to solve dynamic structural problems. Zhong et al. (1996) proposed a so-called ‘‘Subdomain Precise Time Integration Method,’’ which incorporated computational efficiency of the finite difference method to solve both linear and nonlinear dynamic problems. Extending from Tsai and Chuang (2002) that employed the Precise Direct Integration Method (Zhong and Williams, 1994) in combination with numerical kinetic damping to solve static structural problems, this paper adopts Rayleigh damping as a favorable modification for dissipating spurious high frequency responses that oftentimes results from numerical modeling error rather than real structural behavior. The theoretical background of the Precise Integration Method as well as its implementation will be introduced in the following, and its numerical stability and accuracy are thoroughly discussed.

## 2. PRECISE INTEGRATION METHOD FOR SOLVING LINEAR DYNAMICS

### 2.1. Force equilibrium equation of motion

If we assume that  $\ddot{\mathbf{x}}$ ,  $\dot{\mathbf{x}}$  and  $\mathbf{x}$  are acceleration, velocity and displacement vectors, respectively, then most structural dynamic problems of engineering interest, after spatial discretization, can be expressed in the following second order differential equation of motion:

$$\mathbf{M}\ddot{\mathbf{x}} + \mathbf{C}\dot{\mathbf{x}} + \mathbf{K}\mathbf{x} = \mathbf{F} \quad (2.1)$$

in which,  $\mathbf{M}$  is the system mass matrix;  $\mathbf{C}$  is the system damping matrix;  $\mathbf{K}$  is the system stiffness matrix;  $\mathbf{F}$  is the external force or input vector applied to the system. Provided that initial conditions  $\mathbf{x}_0$  and  $\dot{\mathbf{x}}_0$  are known vectors, the governing equation can be rearranged in the following mathematical form:

$$\dot{\mathbf{v}} = \mathbf{A}_c \mathbf{v} + \mathbf{E}_c \mathbf{F} \quad (2.2)$$

in which,

$$\mathbf{v} = \begin{Bmatrix} \mathbf{x} \\ \dot{\mathbf{x}} \end{Bmatrix} \quad (2.3)$$

$$\mathbf{A}_c = \begin{bmatrix} \mathbf{0} & \mathbf{I} \\ -\mathbf{M}^{-1}\mathbf{K} & -\mathbf{M}^{-1}\mathbf{C} \end{bmatrix} \quad (2.4)$$

$$\mathbf{E}_c = \begin{bmatrix} \mathbf{0} \\ \mathbf{M}^{-1} \end{bmatrix} \quad (2.5)$$

$\mathbf{v}$  is the state vector;  $\mathbf{A}_c$  is the time-independent system matrix;  $\mathbf{E}_c$  is the input distribution matrix which is time-independent in this study;  $\mathbf{F}$  is the external force (or input) vector;  $\mathbf{I}$  is the identity matrix or unit matrix. The solution can be obtained by solving Eqn. (2.2) with initial conditions and expressed as:

$$\mathbf{v}(t) = e^{\mathbf{A}_c t} \mathbf{v}_0 + e^{\mathbf{A}_c t} \int_0^t e^{-\mathbf{A}_c s} \mathbf{E}_c \mathbf{F}(s) ds \quad (2.6)$$

The discrete form of Eqn. (2.6) can be expressed as the following form if the external force  $\mathbf{F}$  is linearly interpolated between two consecutive time instants:

$$\mathbf{v}_{n+1} = \mathbf{T} \mathbf{v}_n + \mathbf{E}_0 \mathbf{F}_n + \mathbf{E}_1 \mathbf{F}_{n+1} \quad (2.7)$$

$$\mathbf{E}_0 = \left( \mathbf{A}_c^{-1} \mathbf{T} + \frac{1}{\Delta t} \mathbf{A}_c^{-2} (\mathbf{I} - \mathbf{T}) \right) \mathbf{E}_c \quad (2.8)$$

$$\mathbf{E}_1 = \left( -\mathbf{A}_c^{-1} + \frac{1}{\Delta t} \mathbf{A}_c^{-2} (\mathbf{T} - \mathbf{I}) \right) \mathbf{E}_c \quad (2.9)$$

On the other hand, an arbitrarily degree of nonlinear polynomial function can be used as well; thus, the above expressions for  $\mathbf{E}_0$  and  $\mathbf{E}_1$  will take a different form should the forcing function be nonlinearly interpolated between two consecutive time instants.

$$\mathbf{T} = e^{\mathbf{A}_c \Delta t} = \left( e^{\mathbf{A}_c \Delta t / m} \right)^m = \left( e^{\mathbf{A}_c \tau} \right)^m \quad (2.10)$$

in which  $\tau = \Delta t / m$ . If  $m$  is selected as an integer power of 2 (i.e.,  $m = 2^N$ ) and a fairly large  $N$  value is used (e.g.,  $N = 20$ ), then  $\tau = \Delta t / m$  will be extremely small such that truncation error from higher order terms of Taylor series approximation becomes negligible. With a very small  $\tau$ , the exponential term  $e^{\mathbf{A}_c \tau}$  can be approximated by the higher order Taylor series expansion with satisfactory precision, taking the fourth order expansion for an example:

$$\begin{aligned} e^{\mathbf{A}_c \tau} &\approx \mathbf{I} + \mathbf{A}_c \tau + (\mathbf{A}_c \tau)^2 / 2! + (\mathbf{A}_c \tau)^3 / 3! + (\mathbf{A}_c \tau)^4 / 4! \\ &= \mathbf{I} + \mathbf{T}_a \end{aligned} \quad (2.11)$$

It is noted that the elements in the additional matrix  $\mathbf{T}_a$  are very small as compared to the identity matrix  $\mathbf{I}$ . Substitution of Eqn. (2.11) back into Eqn. (2.10) gives:

$$\mathbf{T} = (\mathbf{I} + \mathbf{T}_a)^m = (\mathbf{I} + \mathbf{T}_a)^{2^N} = (\mathbf{I} + \mathbf{T}_a)^{2^{(N-1)}} (\mathbf{I} + \mathbf{T}_a)^{2^{(N-1)}} \quad (2.12)$$

In Eqn. (2.12), there are  $N$  matrix multiplications of the  $(\mathbf{I} + \mathbf{T}_a)^2$  term, which can be expanded into:

$$(\mathbf{I} + \mathbf{T}_a) \times (\mathbf{I} + \mathbf{T}_a) = \mathbf{I} + 2\mathbf{T}_a + \mathbf{T}_a^2 \quad (2.13)$$

When the exponential matrix  $\mathbf{T}$  is numerically obtained through computer computations, Eqn. (2.13) shall repeatedly multiply itself  $N$  times and this can be readily accomplished by a do loop computer routine. In such a routine, the numerical result of  $2\mathbf{T}_a + \mathbf{T}_a^2$  is stored back into the additional matrix  $\mathbf{T}_a$  each time, and  $\mathbf{T}_a$  must be stored separately from the identity matrix  $\mathbf{I}$  during the computations for better numerical accuracy instead of being directly added to the identity matrix  $\mathbf{I}$ ; otherwise, the loss of numerical accuracy will be significant due to round-off errors. This is because the elements in additional matrix  $\mathbf{T}_a$  are very small as compared to the identity matrix  $\mathbf{I}$ . After  $N$  matrix multiplications,

the elements in  $T_a$  are no longer small numbers such that the addition of  $T_a$  and the identity matrix  $I$  will have no serious numerical round-off error. The algorithm given above is called the precise computation of the exponential matrix as the separate storage of  $I$  and  $T_a$  during the computation process can enhance the resulting numerical accuracy.

## 2.2. Momentum equilibrium equation of motion

If the system  $M$ ,  $C$  and  $K$  remain constant over the time interval of integration, integrating the force equation of motion Eqn. (2.1) with respect to time leads to:

$$M\dot{w} + Cw + Kw = J \quad (2.14)$$

in which,  $\ddot{w} = \int \ddot{x} dt$ ;  $\dot{w} = \int \dot{x} dt$ ;  $w = \int x dt$ ;  $J$  represents the time integral of external force or the external momentum vector during the time interval  $0 \leq \tau \leq t$ . Eqn. (2.12) can be expressed in state space form as follows:

$$\begin{Bmatrix} \dot{w} \\ \ddot{w} \end{Bmatrix} = \begin{bmatrix} 0 & I \\ -M^{-1}K & -M^{-1}C \end{bmatrix} \begin{Bmatrix} w \\ \dot{w} \end{Bmatrix} + \begin{Bmatrix} 0 \\ M^{-1}J \end{Bmatrix} \quad (2.15)$$

Eqn (2.13) can be solved using the Precise Integration Method with exactly the same procedure previously mentioned.

## 3. NUMERICAL STABILITY AND ACCURACY

The Precise Integration Method needs to first assume an  $N$  value in order to calculate the amplification matrix; thus, its numerical stability depends on the  $N$  value used for analysis. Fig. 3.1(a) shows the relations between spectral radius  $\rho$  and  $\Delta t/T$  using the fourth-order Taylor series approximation in case of an undamped SDoF oscillator under free vibration. An algorithm is considered as stable if the numerical solution for free vibration will not grow without bound for any arbitrary initial conditions (i.e., spectral radius  $\rho \leq 1$ .) It can be seen that when the  $N$  value increases, the range of  $\Delta t/T$  for maintaining numerical stability becomes wider. Whenever numerical stability is satisfied, the values of spectral radius are mostly close to 1. On the other hand, the numerical accuracy of an integration method can be evaluated by its relative period error  $(\bar{T} - T)/T$  and fictitious decay of vibration amplitude. The latter can be represented by the so-called algorithmic damping ratio  $\bar{\xi}$ . The influence of both factors depends on the numerical accuracy of eigenvalues calculated from the amplification matrix of the structural model. Assume the calculated eigenvalues of the amplification matrix for an undamped SDoF oscillator are:

$$\lambda_{1,2} = a \pm i|b| = e^{-\bar{\xi}\bar{\omega}_n\Delta t} (\cos \bar{\omega}_n \Delta t \pm i \sin \bar{\omega}_n \Delta t) \quad (3.1)$$

in which,  $i = \sqrt{-1}$ , and  $b \neq 0$ ; Eqn. (3.1) also implies:

$$\bar{\omega}_n \Delta t = \begin{cases} \tan^{-1}(|b|/a) & (a > 0) \\ \tan^{-1}(|b|/a) + \pi & (a < 0) \end{cases} \quad (3.2)$$

$$\bar{\xi} = \frac{-\ln(a^2 + b^2)}{2\bar{\omega}_n \Delta t} \quad (3.3)$$

The relative period error is defined as

$$\frac{\bar{T} - T}{T} = \frac{\omega_n}{\bar{\omega}_n} - 1 = \frac{\omega_n \Delta t}{\bar{\omega}_n \Delta t} - 1 \quad (3.4)$$

in which,  $T$  is the natural period of the structural model;  $\bar{T}$  is the numerical period obtained from the Precise Integration Method;  $\omega_n$  is the circular natural frequency;  $\bar{\omega}_n$  is the circular numerical frequency obtained from the Precise Integration Method.

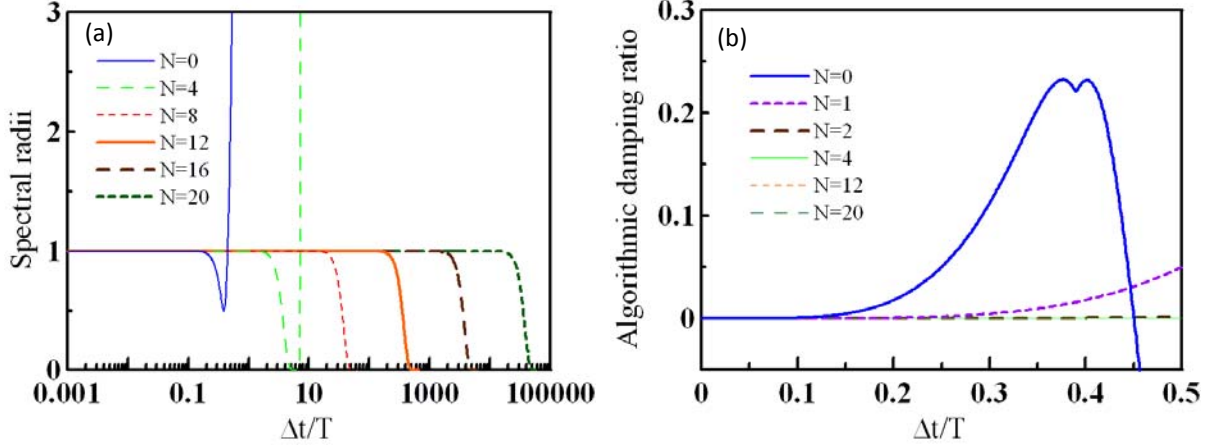


**Figure 3.1.** Relations of spectral radius  $\rho$  vs.  $\Delta t/T$  (left) and  $\bar{\xi}$  vs.  $\Delta t/T$  (right) using the fourth-order Taylor series approximation in the Precise Integration Method.

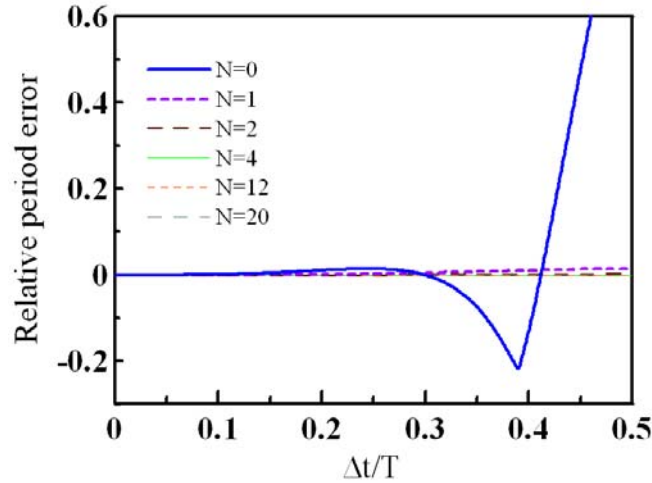


**Figure 3.2.** Relation between  $(\bar{T} - T)/T$  and  $\Delta t/T$  using the fourth-order Taylor series approximation in the Precise Integration Method.

Fig. 3.1(b) shows the relation between algorithmic damping ratio  $\bar{\xi}$  and  $\Delta t/T$  corresponding to different  $N$  values under the fourth-order Taylor series approximation in case of an undamped SDoF oscillator under free vibration. It can be seen from Fig. 3.1(b) that when  $N$  increases, the algorithmic damping ratio decreases. When  $N \geq 4$ ,  $\bar{\xi}$  is approximately zero for  $\Delta t/T = 0 \sim 0.5$ . Fig. 3.2 shows the relation between the relative period error  $(\bar{T} - T)/T$  and  $\Delta t/T$  corresponding to different  $N$  values under the fourth-order Taylor series approximation. It can be seen from Fig. 3.2 that when  $N$  increases, the relative period error decreases substantially; when  $N \geq 1$ , the relative period error is approximately zero for  $\Delta t/T = 0 \sim 0.5$ . It should be noted that  $N=0$  corresponds to the ordinary integration algorithm

using Taylor series expansion integrated in one single time step, which yields minimal algorithmic damping ratio and relative period error only for  $\Delta t/T \leq 0.1$  when the fourth-order Taylor series approximation is used. It can be concluded that the Precise Integration Method yields response results with higher accuracy than the ordinary integration methods if the same time step size is taken in the analyses. In the following discussions, we will find that the combination of  $N=20$  and the fourth-order Taylor series approximation as originally suggested by Zhong et al. (1996) provides an excellent match with its analytical counterpart.

#### 4. INCORPORATION OF SPURIOUS HIGH-FREQUENCY DISSIPATING CAPABILITY

It is well recognized that the accuracy of natural period and mode shape estimates largely depends on the analytical model used for dynamic response analyses; however, even the best estimates of natural periods and mode shapes obtained from a sophisticated structural model may be still slightly deviated from its real life counterpart. As such, oftentimes a numerical model can only well represent the first few vibration modes of the real structure but has larger relative period errors in higher modes; the high frequency responses from a numerical model are most likely spurious, and more or less reduce the accuracy of numerical response analyses. Besides, the spurious high frequency responses may cause numerical instability. As the spurious high frequency response is undesirable and better be removed, a modification is proposed here to enable the Precise Integration Method to get rid of the influence from fictitious high frequency response, and keeps only the most trustworthy response from the first few predominant modes. To reach this goal, an additional damping coefficient matrix  $\mathbf{C}_a$  that is linearly proportional to system stiffness matrix  $\mathbf{K}$  and time step size  $\Delta t$  is incorporated into the Precise Integration Method as follows:

$$\mathbf{C}' = \mathbf{C} + \mathbf{C}_a = \mathbf{C} + 2\alpha \mathbf{K} \Delta t \quad (4.1)$$

in which,  $\mathbf{C}'$  is the modified system damping coefficient matrix;  $\mathbf{C}$  is the original system damping coefficient matrix;  $\alpha$  is the damping modification factor. An appropriate value is specified for damping modification factor  $\alpha$  to dissipate undesirable spurious high frequency response. The eigenvalues of the amplification matrix for an SDoF system after incorporating numerical damping can be expressed as follows:

$$\lambda_{1,2} = \begin{cases} \exp\left(-\xi^* \omega_n \Delta t \pm i \omega_n \Delta t \sqrt{1 - \xi^{*2}}\right) & \text{if } 0 \leq \xi^* < 1 \\ \exp\left(-\xi^* \omega_n \Delta t \pm \omega_n \Delta t \sqrt{\xi^{*2} - 1}\right) & \text{if } \xi^* \geq 1 \end{cases} \quad (4.2)$$

in which  $\xi^* \geq 1$  indicates that the original SDoF system has been changed to become critically or overly damped by the additional numerical damping, and therefore no longer represents a vibratory system. Please note that this mistake is not acceptable and should be avoided. The modified system damping ratio after incorporating Eqn. (4.1) thus takes the following form:

$$\xi^* = \frac{C + 2\alpha K \Delta t}{2M\omega_n} = \xi + 2\alpha\pi \frac{\Delta t}{T} \quad (4.4)$$

Recall that spectral radius  $\rho = \max(|\lambda_1|, |\lambda_2|)$ . If we further assume the SDoF system is free of damping (i.e.,  $\xi = 0$ ) for simplicity, then substitution of Eqn. (4.4) into Eqns. (4.2) and (4.3) will yield the following:

$$\alpha = \begin{cases} -\frac{\ln \rho}{(\omega_n \Delta t)^2} & \text{if } 0 \leq \xi < 1 \\ 1 + \left( \frac{\ln \rho}{\omega_n \Delta t} \right)^2 & \text{if } \xi^* \geq 1 \end{cases} \quad (4.5)$$

$$\alpha = \begin{cases} -\frac{\ln \rho}{(\omega_n \Delta t)^2} & \text{if } 0 \leq \xi < 1 \\ 1 + \left( \frac{\ln \rho}{\omega_n \Delta t} \right)^2 & \text{if } \xi^* \geq 1 \end{cases} \quad (4.6)$$

Fig. 4.1(a) takes an undamped SDoF oscillator under free vibration as an example, and shows the relation between spectral radius and  $\Delta t/T$  corresponding to different  $\alpha$  values. Since the combination of  $N=20$  and the fourth-order Taylor series approximation as originally suggested by Zhong et al. (1996) provides a good match with the analytical exact solution from Eqns. (4.5)-(4.6), only the numerical results are plotted in Fig. 4.1 for better graphical readability. If the cut-off frequency for suitable numerical dissipation and time step size  $\Delta t$  are both decided, then an appropriate  $\alpha$  value can be readily determined using Eqn. (4.5) or Fig. 4.1(a) to help filter out fictitious high frequency response. The  $\alpha$  value can be then fed back into the modified system matrix  $A'_c$  to dissipate undesirable high frequency responses. Fig. 4.1(a) suggests that a larger time step would pair with a smaller damping modification factor  $\alpha$  while a smaller time step would pair with a larger  $\alpha$  value in order to have the same spurious high frequency dissipation effects. A much smaller  $\alpha$  value than Eqn. (4.5) or Fig. 4.1(a) suggests may lead to insufficient dissipation capacity, while a much larger  $\alpha$  value may overly damp out trustworthy low frequency response from the first few predominant vibration modes. The dashed portion of the curves in Fig. 4.1(a) represents  $\xi^* \geq 1$  and will erroneously transform an SDoF oscillator (i.e., under-damped) into a non-vibratory system (i.e., critically or overly damped) and therefore should not be used.

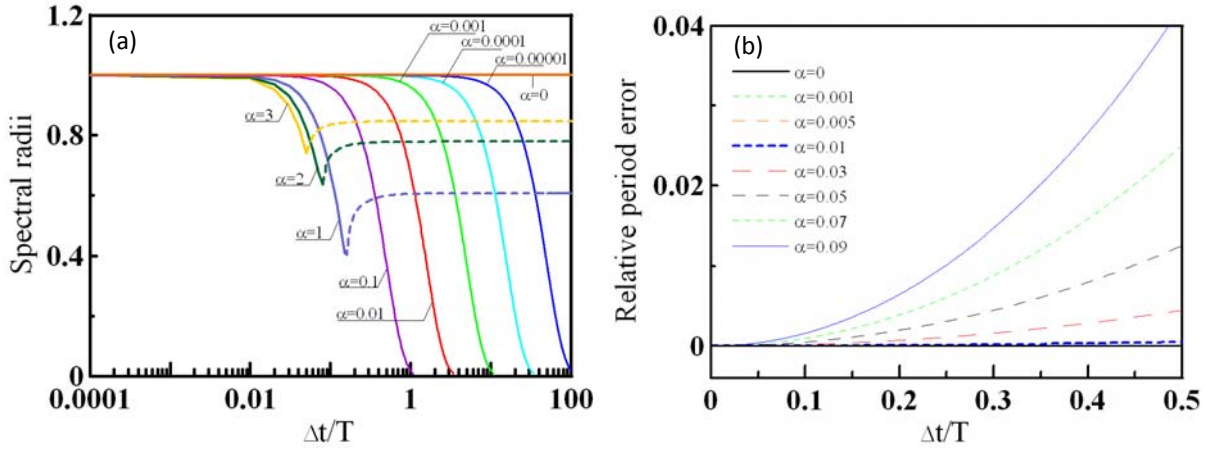


**Figure 4.1.** Relations of spectral radius  $\rho$  vs.  $\Delta t/T$  (left) and  $(\bar{T} - T)/T$  vs.  $\Delta t/T$  (right) using the fourth-order Taylor series approximation and  $N=20$  in the Precise Integration Method.

The relation between the relative period error and  $\Delta t/T$  under different  $\alpha$  values can be shown as Fig. 4.1(b). The curves in Fig. 4.1(b) also agree exceptionally well with the analytical results calculated from Eqn. (3.4). As such, only the numerical results are plotted in Fig. 4.1(b) for better graphical readability. Fig. 4.1(b) suggests that when  $\alpha$  value increases, relative period error also increases. It is therefore suggested that  $\Delta t$  be as large as possible (a larger  $\Delta t$  will not significantly affect the period error too much due to the superior performance from the power-of-two algorithm and the fourth-order Taylor approximation and can help alleviate computational effort) and then select a suitable  $\alpha$  value to dissipate fictitious response as long as numerical stability and accuracy requirement (usually,  $\Delta t/T \leq 0.1$ ) are both satisfied. Ultimately, if the values of  $\alpha$  and  $\Delta t$  are carefully selected, the spurious high frequency response from modeling error can be successfully filtered out, and accurate response prediction from the first few predominant modes can be assured. The excellent match between numerical results and exact solutions in Fig. 4.1 facilitates an equation-based prediction of

resulting numerical characteristics when a combination of  $N=20$  and the fourth-order Taylor series approximation is employed in the Precise Integration Method. The required computational effort of a numerical approach is always a major concern of its users. In case of DOFs = 1000, a 17.4% increase in computational time is observed if  $N$  value increases from 0 to 20, while the computational time grows exponentially with the number of degrees of freedom due to the state space approach employed. In passing, it is mentioned that the additional computational effort induced by the power-of-two algorithm is marginal considering the significant improvement in numerical accuracy.

## 5. ISSUE OF SPURIOUS RESONANCE UNDER FORCED VIBRATIONS

The computational performance of a time integration method for solving linear dynamics problems is usually evaluated with reference to its capability in accurately obtaining the homogeneous part of the solution and numerical stability; however, the influence of external loading has not been studied as widely, and usually limited to the investigation of local truncation error. Cannillo and Mancuso (2000, 2002) performed accuracy analysis on time integration methods for classically damped MDoF linear dynamic oscillating systems using the transfer function that is expressed in terms of an amplification matrix and a loading vector under the assumption of stationary disturbance. The MDoF oscillating system usually can be decomposed into a group of SDoF oscillators using modal decomposition if a classical damping is assumed. When compared with the exact transfer function, numerical accuracy and spurious resonance resulted from a time integration method due to the influence of the external loading can be then evaluated. As a stationary external excitation can always be represented by a superposition of sinusoidal waveforms using exponential Fourier series, the transfer function of an viscously damped linear SDoF oscillating system between a stationary acceleration excitation  $f(t) = \exp(i\Omega t)$  and the resulted system displacement response can be then analytically expressed in the following form according to random vibration theory:

$$H_x = \frac{1}{\omega_n^2 - \Omega^2 + 2i\xi\omega_n\Omega} \quad (5.1)$$

On the other hand, all numerical time integration methods have their own numerically resulted transfer functions that may deviate from the exact form of Eqn. (5.1). If we assume the relation between the external loading and the response vector containing displacement and velocity at a particular time instant  $t_n$  is of the following vector form:

$$\begin{Bmatrix} x_n \\ \dot{x}_n \end{Bmatrix} = \begin{Bmatrix} H_x \\ H_{\dot{x}} \end{Bmatrix} e^{(i\Omega n\Delta t)} \quad (5.2)$$

$H_x$  and  $H_{\dot{x}}$  correspond to the transfer functions for displacement and velocity response of the SDoF structural system, respectively. If we substitute Eqn. (5.2) into Eqn. (2.7), the following expression for transfer function is then obtained from the explicit recursive equation of the Precise Integration Method:

$$\begin{Bmatrix} \bar{H}_x \\ \bar{H}_{\dot{x}} \end{Bmatrix} = [e^{i\Omega\Delta t} \mathbf{I} - \mathbf{T}]^{-1} [\mathbf{E}_0 \quad \mathbf{E}_1] \begin{Bmatrix} 1 \\ e^{i\Omega\Delta t} \end{Bmatrix} \quad (5.3)$$

Eqn. (5.3) can be employed to calculate the transfer functions for the Precise Integration Method. Similarly, both the transfer functions resulted from the original Newmark's and the central difference methods can be obtained following the same procedure. If the forcing-to-system frequency ratio  $\nu$  is defined as the external harmonic excitation frequency  $\Omega$  divided by the system frequency  $\omega_n$ , then the norm of the numerical transfer function normalized with respect to that of the exact transfer function

denoted by  $|\overline{H}_x|/|H_x|$  can be employed to evaluate numerical accuracy and spurious resonance for numerical integration methods. It should be noted that in case of  $|\overline{H}_x|/|H_x|=1$ , the numerical time integration method yields perfectly accurate result as the analytical exact solution. Fig. 5.1 compares numerical accuracy and spurious resonance of several integration methods, including the Precise Integration Method, Newmark's method and the central difference method, within  $0 \leq \nu \leq 2.5$  by assuming an undamped SDoF system of a natural circular frequency  $\omega_n=2$  rad/sec (i.e., natural period  $T = 3.14$ sec). All three methods use a time step  $\Delta t=0.314$ sec  $=0.1*T$ . The parameters  $\gamma = 0.5$  and  $\beta = 0.25$  are assumed in the original Newmark's method, corresponding to the average acceleration method. When the forcing-to-system frequency ratio  $\nu$  is much smaller than 1 (in particular, smaller than 0.7), all three integration methods yield response fairly close to the exact solution; however, both the central difference and the original Newmark's (average acceleration) methods show unfavorable spurious resonance with abrupt vertical spikes when the forcing-to-system frequency ratio  $\nu$  is in the vicinity of 1. When the forcing-to-system frequency ratio  $\nu$  is larger than the value causing spurious resonance in the central difference and the original Newmark's methods, the numerical-to-exact transfer function ratio starts to deviate away from 1. For larger time step sizes tested in this study, the spurious resonance problem becomes catastrophically worse, and can result in a large half-power bandwidth at spurious resonance such that the resulting numerical accuracy substantially degrades and becomes unacceptable. The accuracy of the Precise Integration Method also degrades if an excessively large time step is taken (e.g.,  $\Delta t > 0.3*T$ ). Fig. 5.2(a) plots the numerical accuracy of the Precise Integration Method with the forcing function linearly interpolated within an integration time step. The curves shown cover a good spectrum of  $\Delta t/T$  values (1/100, 1/40, 1/20, and 1/10), corresponding to  $\omega_n = 0.2, 0.5, 1,$  and  $2$  rad/sec. The parametric study indicates that although spurious resonance does not exist in the Precise Integration Method, its overall numerical accuracy degrades when the structural and/or forcing frequency grows higher. Fig. 5.2(b) reports the advantage of employing a second-degree polynomial in describing the variation of loading momentum within integration time steps, which shows substantially improved accuracy. Numerical example study shows that the use of nonlinear polynomials can further loosen the constraint of time step size selection but still keeps the desired level of numerical accuracy at the same time.

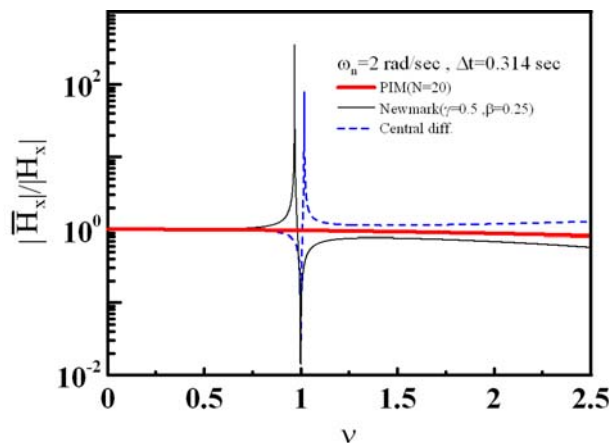


**Figure 5.1.**  $|\overline{H}_x|/|H_x|$  vs.  $\nu$  relations obtained from the central difference, the original Newmark's and the Precise Integration Methods ( $\zeta = 0$ ,  $\Delta t = 0.314$ sec  $= 0.1*T$ ).

## 7. CONCLUSIONS

An explicit time integration method capable of dissipating spurious high frequency responses is proposed in the study, which is a modified version of the original Precise Integration Method. From numerical stability and accuracy analyses, it is found that when the  $N$  value reaches a certain threshold (e.g.,  $N \geq 20$ ) and the fourth-order Taylor series approximation is employed, the Precise Integration Method becomes almost unconditionally stable over a wide range of frequencies and its accuracy is

better than most commonly used integration methods in the engineering community. The power-of-two algorithm and Taylor series expansion are both well known mathematical concept in textbooks, so the authors trust that its end users will be able to get familiar with the approach more easily compared with other state-of-the-art methods having been proposed in the literature, while the Precise Integration Method still provides competitively excellent numerical stability and accuracy. The next mission of the study in the near future is to take a step further to investigate the possibility of extending to materially nonlinear systems and carefully evaluate its numerical performance.

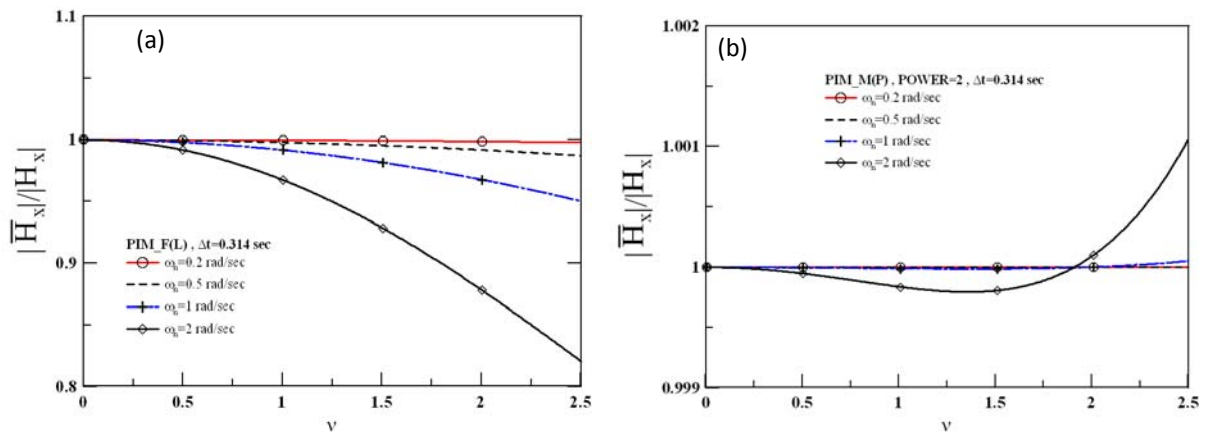


**Figure 5.2.**  $|\bar{H}_x|/|H_x|$  vs.  $\nu$  relations obtained from force (left) and momentum (right) equilibrium of the Precise Integration Method under various structural natural frequencies ( $\Delta t=0.314$ sec,  $\omega_n=1\sim 5$  rad/sec).

## ACKNOWLEDGEMENT

The study reported here was funded in part by the National Science Council of Taiwan under grant number NSC95-2221-E-033-062. This financial support is gratefully acknowledged. All opinions expressed in this paper are solely those of the authors and do not necessarily represent the views of the sponsor.

## REFERENCES

- Cannillo, V. and Mancuso, M. (2002). Spurious resonances in numerical time integration methods for linear dynamics. *J. of Sound and Vibration* **238**: 3, 389-399.
- Cannillo, V. and Mancuso, M. (2002). On the behavior of dissipative time integration methods near the resonance condition. *J. of Sound and Vibration* **249**: 3, 599-605.
- Chien, C.C., Chen, Y.H., Chuang C.C. (2003). Dual reciprocity BEM analysis of 2-D transient elastodynamic problems by time-discontinuous Galerkin FEM, *Engineering Analysis with Boundary Elements*, **27**, 611-624.
- Hughes, T.J.R. (1987). *The finite element method: linear static and dynamic finite element analysis*, Prentice-Hall, Englewood Cliffs, NJ.
- Lin, J., Shen, W., Williams, F.W. (1995). A high precision direct integration scheme for structures subjected to transient dynamic loading, *Comput Struct* **56**, 113-120.
- Shen, W., Lin, J., Williams, F.W. (1995). Parallel computing for high precision direct integration method. *Comput Meth Appl Mech Engrg* **126**, 315-331.
- Subbaraj, K. and Dokainish, M.A. (1989). A survey of direct time-integration method in computational structural dynamic - I. Explicit methods, *Comput Struct* **32**, 1371-1386.
- Subbaraj, K. and Dokainish, M.A. (1989). A survey of direct time-integration method in computational structural dynamic - II. Implicit methods, *Comput Struct* **32**, 1387-1401.
- Tsai, M.C. and Chuang, C.C. (2002). An application of precision integration method in structure static and dynamic problems, in: *Proceedings of 6th National Conference on Structural Engineering*, Taiwan, Paper No. F19 (in Chinese.)
- Zhong, W.X. and Williams, F.W. (1994). A precise time step integration method. *Proceedings of the Institution of Mechanical Engineers*. **208**: 427-430.
- Zhong, W.X., Zhu, J., Zhong, X.X. (1996). On a new time integration method for solving time dependent partial differential equations. *Comput Meth Appl Mech Engrg* **130**, 163-178.